PHYSICAL REVIEW B **81**, 060508(R) (2010)

Anomalous Nernst effect and heat transport by vortex vacancies in granular superconductors

Andreas Andersson* and Jack Lidmar†
Theoretical Physics, Royal Institute of Technology, AlbaNova, SE-106 91 Stockholm, Sweden
(Received 25 November 2009; published 24 February 2010)

We study the Nernst effect due to vortex motion in two-dimensional granular superconductors using simulations with Langevin or resistively shunted Josephson-junction dynamics. In particular, we show that the geometric frustration of both regular and irregular granular materials can lead to thermally driven transport of vortices from colder to hotter regions, resulting in a sign reversal of the Nernst signal. We discuss the underlying mechanisms of this anomalous behavior in terms of heat transport by mobile vacancies in an otherwise pinned vortex lattice.

DOI: 10.1103/PhysRevB.81.060508 PACS number(s): 74.81.−g, 74.25.F−, 74.25.Uv, 74.78.−w

The Nernst effect—the generation of a transverse voltage when a temperature gradient is applied to a metal or superconductor placed in a perpendicular magnetic field—has become an important experimental probe of correlation effects. For example, recent experiments on high-T_c cuprates[1] and conventional superconducting films[2] have found a remarkably strong Nernst signal in a wide regime above the critical temperature. Being small in most ordinary metals, the Nernst effect is naturally attributed to superconducting fluctuations, either of Gaussian nature[3–5] or due to vortex fluctuations.[1,6,7] In the case of granular superconductors, the added complication of geometric frustration may significantly affect transport properties. Here, we show that anomalous sign reversals of the Nernst signal can appear in such systems, as the magnetic field is varied.

Let us define a geometry with a perpendicular magnetic field B_z and a temperature gradient $-\nabla_x T$ inducing an electric field E_y. The Nernst signal e_N and the Nernst coefficient ν are then defined by

$$\nu = \frac{e_N}{B_z} = \frac{1}{B_z}\frac{E_y}{(-\nabla_x T)}. \tag{1}$$

In metals the Nernst effect is typically small, being proportional to particle-hole asymmetry, and ν can be either positive or negative.[8] The sign convention adopted here conforms with that used in the recent literature.[1,3–8] In type-II superconductors, the Nernst effect is usually much stronger. There, field-induced vortices diffusing down the applied temperature gradient will generate a transverse electric field $\mathbf{E}=\mathbf{B}\times\mathbf{v}$, where the drift velocity of the vortices is $\mathbf{v}=\nu(-\nabla T)$, leading to $\mathbf{E}=\nu\nabla T\times\mathbf{B}$. The vortex Nernst effect is thus a diagonal response of the *vortex* current to a temperature gradient. Notably, the sign of ν is *positive* if vortices are driven down the temperature gradient from hotter to colder regions. The only way to obtain a *negative* value of ν from the vortex motion is then if a situation arises in which vortices move from colder to hotter regions, against the thermal gradient. A complementary point of view is provided by an Onsager relation, relating the Nernst signal e_N and the heat current response J_x^Q to an applied electric current J_y, so that $J_x^Q = Te_N J_y$. It follows that $J_x^Q = Te_N\sigma_{yy}B_z v_x$, which shows that a negative Nernst signal (for $B_z>0$) implies heat flow in the direction opposite that of vortex motion. In this Rapid Communication we show that such anomalous behavior can indeed be realized in granular superconductors.

Consider first a regular two-dimensional Josephson-junction array in a magnetic field corresponding to a commensurate filling of flux quanta. At low enough temperatures the vortices will then form a regular lattice commensurate with the array. For example, at half-filling $f=1/2$ on a square lattice, the vortices will order in a checkerboard pattern. If the density of vortices is lowered slightly below this filling, vacancies are introduced into the system and, in the absence of any pinning, these will be mobile. An applied temperature gradient could then produce a drift of these vacancies from hotter to colder regions, resulting in a net vortex flow in the opposite direction and consequently a negative Nernst signal.

We have confirmed this scenario by numerical simulations in regular arrays (see Figs. 1 and 2 below). Our results show that a negative Nernst signal also can appear in moderately random Josephson-junction networks. We have used two different models for the dynamics of the arrays: (i) Langevin dynamics and (ii) resistively shunted Josephson-junction (RSJ) dynamics. The former corresponds to overdamped model-*A* dynamics,[9] while the latter takes into account cur-

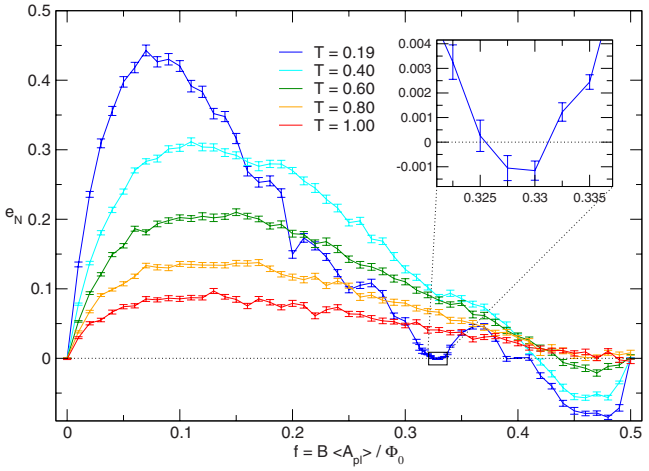

FIG. 1. (Color online) Nernst signal e_N versus filling fraction f for a 20×20 square lattice at different temperatures T. Notice how the Nernst signal goes clearly negative in the region $0.4\lesssim f\lesssim 0.5$. Inset: zoom-in of e_N at $T=0.19$ around $f=1/3$, where e_N also becomes negative.

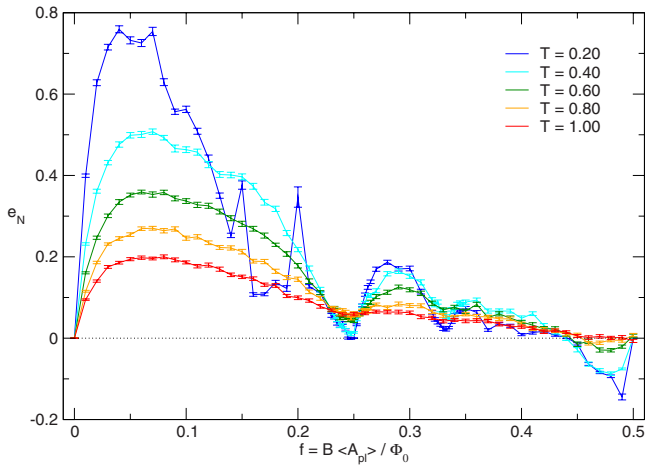

FIG. 2. (Color online) Nernst signal e_N versus filling fraction f for a 20×20 triangular lattice at different temperatures T. Here, e_N shows more structure as a function of f, but again becomes clearly negative for f between 0.4 and 0.5.

rent conservation (but neglects charging effects, i.e., no grain or intergrain capacitance). Previous simulations have been based on time-dependent Ginzburg-Landau dynamics,[4] which take into account fluctuations of the amplitude of the order parameter, and Langevin dynamics,[6] equivalent to the model we use but with different boundary conditions.

For both Langevin and RSJ dynamics the supercurrent flowing between two superconducting grains is given by

$$I_{ij}^s = I_{ij}^c \sin(\theta_i - \theta_j - A_{ij}), \quad A_{ij} = \frac{2\pi}{\Phi_0}\int_{\mathbf{r}_i}^{\mathbf{r}_j} \mathbf{A}\cdot d\mathbf{r}, \tag{2}$$

where I_{ij}^c is the critical current of the junction, $\Phi_0 = h/2e$ is the superconducting flux quantum, θ_i is the superconducting phase of grain i, and $\mathbf{A}$ is the magnetic vector potential. We will take $\mathbf{A} = \mathbf{A}_{\text{ext}} + (\Phi_0/2\pi)\boldsymbol{\Delta}$, where $\mathbf{A}_{\text{ext}}$ is constant in time and corresponds to a uniform magnetic field $\mathbf{B} = \nabla\times\mathbf{A}$ perpendicular to the array, and $\boldsymbol{\Delta} = (\Delta_x, \Delta_y)$ is time dependent but spatially uniform, describing fluctuations in the electric field $\mathbf{E} = -\dot{\mathbf{A}} = -(\Phi_0/2\pi)\dot{\boldsymbol{\Delta}}$.[10] For Langevin dynamics the equation of motion is

$$\gamma\dot{\theta}_i = -\frac{1}{2e}\sum_{j\in\mathcal{N}_i} I_{ij}^s + \eta_i, \tag{3}$$

where η_i is a Gaussian white noise with correlations $\langle\eta_i\rangle = 0$ and $\langle\eta_i(t)\eta_j(t')\rangle = (2k_BT\gamma/\hbar)\delta_{ij}\delta(t-t')$. The sum runs over the set $\mathcal{N}_i$ of superconducting grains connected to i. An additional equation describes the dynamics of the twists $\boldsymbol{\Delta}$,[10]

$$\gamma_\Delta\dot{\boldsymbol{\Delta}} = \frac{1}{2e}\sum_{\langle ij\rangle} I_{ij}^s \mathbf{r}_{ji} + \boldsymbol{\zeta}, \tag{4}$$

with a time constant $\gamma_\Delta = \gamma L_x L_y$ and $\langle\boldsymbol{\zeta}(t)\rangle = 0$, $\langle\zeta_\mu(t)\zeta_\nu(t')\rangle = (2k_BT\gamma_\Delta/\hbar)\delta_{\mu\nu}\delta(t-t')$. Here, the sum runs over all junctions in the network and $\mathbf{r}_{ji} = \mathbf{r}_j - \mathbf{r}_i$.

For RSJ dynamics every Josephson junction is shunted by a resistor R, leading to a total current from i to j,

$$I_{ij}^{\text{tot}} = I_{ij}^s + \frac{V_{ij}}{R} + I_{ij}^n, \tag{5}$$

where V_{ij} is the voltage across the junction, given by the ac Josephson relation,

$$V_{ij} = \frac{\Phi_0}{2\pi}(\dot{\theta}_i - \dot{\theta}_j - \dot{A}_{ij}). \tag{6}$$

The Johnson-Nyquist noise in each resistor obeys $\langle I_{ij}^n(t)\rangle = 0$ and $\langle I_{ij}^n(t) I_{kl}^n(t')\rangle = (2k_BT/R)(\delta_{ik}\delta_{jl} - \delta_{il}\delta_{jk})\delta(t-t')$. The equations of motion are obtained from current conservation at each grain, and from the expression for the average total current

$$\sum_{j\in\mathcal{N}_i} I_{ij}^{\text{tot}} = 0, \quad \sum_{\langle ij\rangle} I_{ij}^{\text{tot}}\mathbf{r}_{ji} = L_x L_y \bar{\mathbf{J}}^{\text{ext}}. \tag{7}$$

This gives a system of coupled differential equations for $\{\theta_i\}$ and $\boldsymbol{\Delta}$. We assume periodic boundary conditions in every direction above, with a fixed average current density $\bar{\mathbf{J}}^{\text{ext}}$. For open boundary conditions the fluctuating twist Δ is redundant and should be set to zero in the corresponding direction.

Temperature enters only via the noise correlations and gets a spatial dependence in the presence of a temperature gradient. This allows us to calculate the response of the system to a temperature gradient. Note that the voltage across the system is obtained directly in the simulation from $E_y = -(\Phi_0/2\pi)\dot{\Delta}_y$. It is also possible to calculate the linear response via a Kubo formula,

$$e_N = \frac{L_x L_y}{2k_BT^2}\int_{-\infty}^{\infty}\langle E_y(t) J_x^Q(0)\rangle dt, \tag{8}$$

where the average heat current density is given by

$$J_x^Q = \frac{1}{L_x L_y}\frac{\Phi_0}{2\pi}\sum_{\langle ij\rangle}\left(x_{ji}\frac{1}{2}(\dot{\theta}_i + \dot{\theta}_j) - x_{ij}^c\dot{A}_{ij}\right)I_{ij}, \tag{9}$$

with $x_{ji} = x_j - x_i$ and $x_{ij}^c = (x_i + x_j)/2$. For Langevin dynamics I_{ij} denotes the supercurrent only, while for RSJ dynamics it is the total current (5).[11] Since the temperature is, by necessity, uniform when using the Kubo formula it is possible to employ periodic boundary conditions in this case to eliminate surface effects. Notice that the formulation given above is independent of the lattice structure. We consider here square, triangular, and random lattices.

One may think of a disordered granular thin film as consisting of a random packing of variable sized grains. Every grain is connected to each of its neighbors via a tunnel junction with a critical current I_{ij}^c. Thus, we end up with a randomly connected array of Josephson junctions. We model this by generating a random set of points with unit density in a square, subject to the condition that their separation is larger than some given number $d_{\min}$. Different values of $d_{\min}$ give different levels of heterogeneity, with different widths in the distribution of grain-size diameters. Nearest neighbors are connected via a Delaunay triangulation, with the grains as the corresponding Voronoi cells. Some examples are shown in Fig. 3 with a heterogeneity varying from 7% to 28%.

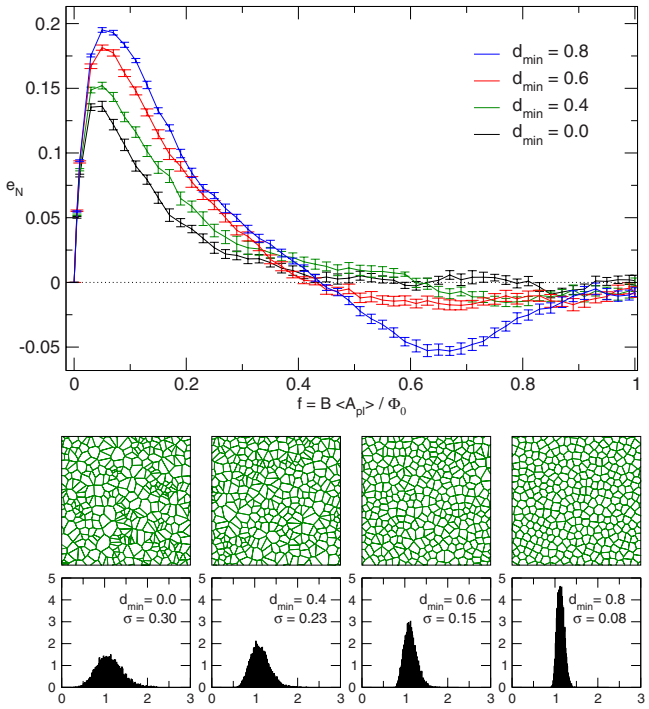

FIG. 3. (Color online) Top: Nernst signal e_N versus filling fraction f at $T=1$ for 20×20 random lattices with different values of the parameter $d_{\min}$. Each curve is an average over 16 disorder realizations. Bottom: examples of lattice structure and size (diameter) distribution of the grains for different values of $d_{\min}$. The grain-size standard deviation σ is also given in each histogram.

The equations of motion, Eqs. (3) and (4) for Langevin dynamics and Eq. (7) for RSJ dynamics, are solved numerically using a forward Euler discretization with time steps of $\Delta t=0.02$ and 0.04, respectively. Note that although we use a forward Euler scheme to integrate the dynamical variables, it is crucial to use a *symmetric* discretization for the heat current J_x^Q.[11] For Langevin dynamics the sampling time is set to $20\times10^6\Delta t$, after a warm-up of $2\times10^6\Delta t$, while the corresponding figures are $10\times10^6\Delta t$ and $1\times10^6\Delta t$ for RSJ dynamics. In addition the results are averaged over 64 or more independent runs. We consider systems with periodic boundary conditions in both directions with sizes up to 160×160, but since finite-size effects are negligible for systems larger than 20×20, only results for this particular system size are presented here. The Nernst signal e_N is calculated from equilibrium fluctuations using the Kubo formula (8), while setting $\bar{\mathbf{J}}^{\text{ext}}=0$. The validity of Eq. (9) and the discretization used is confirmed by checking that the two ways of calculating e_N (Kubo formula and response to a thermal gradient) are consistent. We also verify that the same result is obtained from the response of the heat current to an applied electric current, via an Onsager relation. Temperature is measured in units of the Josephson temperature $E_J/k_B=I^c\Phi_0/2\pi k_B$, and the Nernst signal e_N is given in units of $k_B/2e\gamma$ and $2\pi k_BR/\Phi_0$ for Langevin and RSJ dynamics, respectively. In the majority of our simulations we use Langevin dynamics since it is computationally less expensive and gives qualitatively the same behavior (see Fig. 4 below). Unless otherwise stated, the results below are for Langevin dynamics.

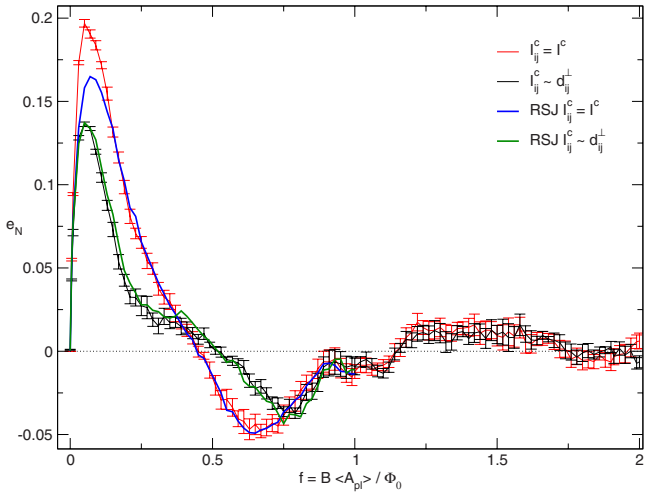

FIG. 4. (Color online) Comparison of the Nernst signal e_N versus filling fraction f between RSJ and Langevin dynamics, and between models with critical currents $I_{ij}^c=I^c$ and $I_{ij}^c\sim d_{ij}^\perp$ for a 20×20 random lattice with $d_{\min}=0.8$ at $T=1$. Each curve is an average over eight disorder realizations. (The RSJ data extend only up to $f=1$.)

Figure 1 shows the Nernst signal e_N as a function of filling $f=B\langle A_{\text{pl}}\rangle/\Phi_0$ for a square lattice ($\langle A_{\text{pl}}\rangle$ is the average plaquette area). The different curves correspond to different temperatures. At low filling a sharp increase culminating in a maximum around $f=0.05-0.15$, depending on temperature, is observed. This is followed by a decrease in the Nernst signal up to half-filling. The tilted-hill profile at high temperatures resembles experimental data of bulk superconductors.[1,2] However, for low temperatures the curves have significant structure due to geometric frustration as the filling is varied through different commensurate values. In particular, notice the sign reversal of e_N just below half-filling. The inset shows a blowup of the region close to another commensurate filling $f=1/3$, where yet another such a region of negative Nernst signal appears, albeit only in a very small parameter regime.

This anomalous sign of the Nernst signal close to, but below, commensurate fillings such as $f=1/3$ and 1/2 can be connected to the large rigidity (i.e., a relatively high melting temperature) of the vortex lattice there. This means that as temperature is raised, the vacancy defect lattice will melt first, while the vortices remain pinned to the underlying lattice. The vacancies can then diffuse down the temperature gradient, resulting in an opposite net vortex flow. Raising the temperature further will eventually melt also the vortex lattice, restoring a positive Nernst signal. It is reasonable to expect that also other regions of negative Nernst signal will show up in narrow parameter windows at low temperatures, just below different commensurate fillings. This scenario of melting transitions has been observed in simulations of square Josephson-junction arrays at $f=5/11\approx0.455$.[12] Furthermore, the rich structure of e_N is reminiscent of the structure of the resistance as a function of f seen in both simulations[13] and in recent experiments[14] on square Josephson-junction arrays.

For a triangular lattice (see Fig. 2) e_N displays a similar

behavior as a function of f, but here the structure due to geometric frustration effects is even more pronounced. The Nernst signal goes once again clearly negative in a region just below half-filling and is strongly suppressed around several other fillings, e.g., $f=1/4$ and 1/3. The relative size of the negative Nernst signal ($\sim 20\%$) is more or less the same compared to the square lattice case.

Note that for perfectly regular arrays the Nernst signal is periodic, with a period of 1, as a function of filling. Furthermore, there is a vortex-vacancy symmetry around half-filling, so that $e_N(f)=-e_N(1-f)$, i.e., the Nernst signal is naturally negative over large regions of $0.5<f<1$ (not shown in the figures). For random networks these properties are absent, and it is not *a priori* clear that the oscillatory behavior with filling persists. Figure 3 displays simulation results of the Nernst signal versus filling for a couple of different random lattices with varying levels of heterogeneity at fixed temperature $T=1$. As seen, most of the structure found in regular lattices is now gone. The same is true also for lower temperatures. There is still a sharp increase at low fillings, reaching a maximum around $f=0.05$, followed by a smooth decay with increasing f. A negative region appears in the most ordered samples ($d_{\min}=0.8$, $\sigma=0.08$) for fillings $0.4 \lesssim f \lesssim 1$. When increasing the geometric disorder by decreasing $d_{\min}$ the region gets smaller, but it is still visible up to at least $d_{\min}=0.4$, $\sigma=0.23$. As the filling is increased further, a weak oscillatory tendency can be seen (Fig. 4). These sign reversals appear to be remnants of the natural periodic behavior of regular structures, but with an amplitude which is quickly damped as filling or disorder is increased.

For granular superconductors RSJ dynamics should give a more realistic microscopic description of fluctuations compared to the phenomenological Langevin dynamics. In Fig. 4 we compare results obtained using Langevin and RSJ dynamics. The curves are essentially identical in the interesting parameter regime where frustration effects are present. The same figure also shows the results for a model where the critical currents of the junctions are taken proportional to the contact area between the grains [or contact length $d_{ij}^{\perp}$ in two dimensions, where $d_{ij}^{\perp}$'s are the bond lengths of the dual (Voronoi) lattice drawn in Fig. 3]. Here, the difference is quantitatively larger, but the qualitative features remain. This indicates that the geometric frustration dominates the Nernst effect and that current conservation and model details are less important in this region.

In conclusion, we have studied the Nernst effect in granular superconductors using a phase only model with Langevin and RSJ dynamics. At low magnetic fields the Nernst signal displays a characteristic tilted-hill profile qualitatively similar to experimental findings.[1,2] For stronger magnetic fields in regular or weakly irregular arrays, we have found regions of anomalous sign changes of the Nernst signal, which translates into sign changes of the Nernst coefficient $\nu=e_N/B_z$. This is contrary to the common belief that the vortex contribution to the Nernst coefficient is always positive. A negative Nernst coefficient implies a net vortex flow from colder to hotter regions and consequently a change in the dominant carriers of heat in the system—from vortices to vortex vacancies. Therefore, the Nernst effect offers a unique way to probe the nature of heat carriers in superconducting structures. We predict that sign reversals of the Nernst signal can be seen in experiments on artificial regular Josephson-junction arrays as well as in granular superconducting thin films at the appropriate magnetic fields.

Support from the Swedish Research Council (VR) and Parallelldatorcentrum (PDC) is gratefully acknowledged.

*anan02@kth.se

†jlidmar@kth.se

[1] Y. Wang, L. Li, and N. P. Ong, Phys. Rev. B **73**, 024510 (2006).

[2] A. Pourret, P. Spathis, H. Aubin, and K. Behnia, New J. Phys. **11**, 055071 (2009).

[3] I. Ussishkin, S. L. Sondhi, and D. A. Huse, Phys. Rev. Lett. **89**, 287001 (2002).

[4] S. Mukerjee and D. A. Huse, Phys. Rev. B **70**, 014506 (2004).

[5] M. N. Serbyn, M. A. Skvortsov, A. A. Varlamov, and V. Galitski, Phys. Rev. Lett. **102**, 067001 (2009).

[6] D. Podolsky, S. Raghu, and A. Vishwanath, Phys. Rev. Lett. **99**, 117004 (2007).

[7] S. Raghu, D. Podolsky, A. Vishwanath, and D. A. Huse, Phys. Rev. B **78**, 184520 (2008).

[8] A. Larkin and A. Varlamov, *Theory of Fluctuations in Superconductors* (Oxford University Press, New York, 2009).

[9] P. C. Hohenberg and B. I. Halperin, Rev. Mod. Phys. **49**, 435 (1977).

[10] B. J. Kim, P. Minnhagen, and P. Olsson, Phys. Rev. B **59**, 11506 (1999).

[11] A. Andersson and J. Lidmar (unpublished).

[12] M. Franz and S. Teitel, Phys. Rev. B **51**, 6551 (1995).

[13] S. Teitel and C. Jayaprakash, Phys. Rev. Lett. **51**, 1999 (1983).

[14] I.-C. Baek, Y.-J. Yun, J.-I. Lee, and M.-Y. Choi, Phys. Rev. B **72**, 144507 (2005).